The Journal of Immunology

Resting and Activation-Dependent Ion Channels in Human Mast Cells

S. Mark Duffy, Wendy J. Lawley, Edward C. Conley and Peter Bradding

J Immunol 2001; 167:4261-4270; ;
doi: 10.4049/jimmunol.167.8.4261
http://www.jimmunol.org/content/167/8/4261

The Journal of Immunology is published twice each month by
The American Association of Immunologists, Inc.,
1451 Rockville Pike, Suite 650, Rockville, MD 20852

Print ISSN: 0022-1767 Online ISSN: 1550-6606.

Resting and Activation-Dependent Ion Channels in Human Mast Cells[1]

S. Mark Duffy, Wendy J. Lawley, Edward C. Conley, and Peter Bradding[2]

The mechanism of mediator secretion from mast cells in disease is likely to include modulation of ion channel activity. Several distinct Ca^{2+}, K^+, and Cl^- conductances have been identified in rodent mast cells, but there are no data on human mast cells. We have used the whole-cell variant of the patch clamp technique to characterize for the first time macroscopic ion currents in purified human lung mast cells and human peripheral blood-derived mast cells at rest and following IgE-dependent activation. The majority of both mast cell types were electrically silent at rest with a resting membrane potential of around 0 mV. Following IgE-dependent activation, >90% of human peripheral blood-derived mast cells responded within 2 min with the development of a Ca^{2+}-activated K^+ current exhibiting weak inward rectification, which polarized the cells to around −40 mV and a smaller outwardly rectifying Ca^{2+}-independent Cl^- conductance. Human lung mast cells showed more heterogeneity in their response to anti-IgE, with Ca^{2+}-activated K^+ currents and Ca^{2+}-independent Cl^- currents developing in ~50% of cells. In both cell types, the K^+ current was blocked reversibly by charybdotoxin, which along with its electrophysiological properties suggests it is carried by a channel similar to the intermediate conductance Ca^{2+}-activated K^+ channel. Charybdotoxin did not consistently attenuate histamine or leukotriene C_4 release, indicating that the Ca^{2+}-activated K^+ current may enhance, but is not essential for, the release of these mediators. ***The Journal of Immunology*****, 2001, 167: 4261–4270.**

Mast cells play a significant role in the pathophysiology of many diverse diseases including asthma and allergy, rheumatoid arthritis, and pulmonary fibrosis through the sustained secretion of numerous proinflammatory mediators including autacoids, cytokines, and proteases (1, 2). The mechanism of mast cell activation in chronic disease is unknown but may reflect continuing exposure to Ag, activation by other inflammatory cell types, or intrinsic abnormalities in the signal transduction pathway for mediator release. Irrespective of the mechanism(s) giving rise to "hypersecretory" states, we hypothesize that all mechanisms will change the activity of the final effector ion channels involved in normal stimulus-secretion coupling. It is therefore important to identify these critical molecular effectors of human mast cell secretion.

IgE-dependent activation of both human and rodent mast cells is characterized by an influx of extracellular Ca^{2+}, which is essential for subsequent release of both preformed (granule-derived) mediators and newly generated autacoids and cytokines. However, flow of ions such as K^+ and Cl^- are likely to play an important role in activation responses because they regulate cell membrane potential and thus influence Ca^{2+} influx (3). For example, in T cells, specific inhibition of the voltage-dependent K^+ channel Kv1.3 by the scorpion toxin margatoxin inhibits their proliferation, IL-2 secretion, and hence delayed-type hypersensitivity responses (4).

Several ion currents have been identified in rodent mast cells, but the function of most of these remains unclear. In both the rat basophilic leukemia (RBL)[3] cell line (RBL-2H3) , a model of mucosal mast cells, and rat IL-3-dependent bone marrow-derived mast cells (BMMC), an inwardly rectifying K^+ channel (Kir) is open when the cells are at rest (5, 6). This channel, which is considered to be Kir2.1 (7), induces a resting membrane potential of approximately −70 mV. Activation-dependent currents have been identified in response to various secretagogues, including a nonselective cation current carrying Ca^{2+} and Na^+ (8), specific Ca^{2+} influx through store-operated calcium channels (SOCC) (9), and an outwardly rectifying Cl^- conductance (10). Adenosine activates an outwardly rectifying K^+ channel in a GTP-dependent and pertussis toxin-sensitive manner which may explain adenosine-potentiated IgE-dependent degranulation (11).

Despite these observations, there are important differences between rodent and human mast cells with respect to mediator content and secretory and pharmacological responsiveness; therefore, from a clinical perspective it is essential that studies be performed on human cells. We have recently identified a voltage-dependent Cl^- current and Ca^{2+}-activated Cl^- and K^+ currents in the human mast cell line HMC-1 (12), but these cells are immature and lack high-affinity IgE receptors and are therefore unsuitable for studying mechanisms of IgE-mediated mast cell degranulation. In this study, we describe for the first time ion currents present at rest and following IgE-dependent activation in human lung mast cells (HLMC) and primary human mast cells derived from progenitors in adult peripheral blood (human peripheral blood-derived mast cells (HPBDMC)). In addition, we have performed a preliminary investigation into the role of a calcium-activated K^+ current (K_{CA}) in IgE-dependent mast cell secretion.

Division of Respiratory Medicine, Institute for Lung Health, University of Leicester, Leicester, United Kingdom

Received for publication January 13, 2001. Accepted for publication August 14, 2001.

The costs of publication of this article were defrayed in part by the payment of page charges. This article must therefore be hereby marked *advertisement* in accordance with 18 U.S.C. Section 1734 solely to indicate this fact.

[1] This work was supported by the Wellcome Trust.

[2] Address correspondence and reprint requests to Dr. Peter Bradding, Department of Respiratory Medicine, Glenfield Hospital, Leicester, LE3 9QP, U.K. E-mail address: pbradding@hotmail.com

[3] Abbreviations used in this paper: RBL, rat basophilic leukemia; HLMC, human lung mast cell; HPBDMC, human peripheral blood-derived mast cell; BMMC, bone marrow-derived mast cell; RPMC, rat peritoneal mast cell; K_{CA}, Ca^{2+}-activated K^+ channel; SOCC, store-operated Ca^{2+} channels; hIKCA1, human intermediate conductance Ca^{2+}-activated K^+ channel; Kir, inwardly rectifying family of K^+ channels; ChTX, charybdotoxin; LTC_4, leukotriene C_4; NPPB, 5-nitro-2-(3-phenylpropylamino)benzoic acid; DIDS, 4,4′-diisothiocyanato-2,2′-disulfonic acid; SCF, stem cell factor.

0022-1767/01/$02.00

Materials and Methods

Reagents

The following were purchased: Stem cell factor (SCF), IL-6, IL-10 (R&D Systems, Abingdon, U.K.); charybdotoxin (ChTX), Histopaque 1077, 2-ME, EGTA (Sigma, Poole, Dorset, U.K.), human myeloma IgE (Calbiochem-Novabiochem, Nottingham, U.K.), sheep polyclonal antihuman IgE (Serotec, Kidlington, Oxford, U.K.), mouse IgG1 mAb YB5B8 (anti-CD117; Cambridge Bioscience, Cambridge, U.K.), sheep anti-mouse IgG1 Dynabeads (Dynal, Wirral, U.K.); histamine, *S*-adenosyl-L-[*methyl*-^{3}H]methionine (Amersham Life Science, Little Chalfont, Buckshire, U.K.), RPMI 1640/Glutamax/HEPES, antibiotic/antimycotic solution, MEM nonessential amino acids, and FCS (Life Technologies, Paisley, U.K.). Rat kidney histamine methyltransferase was a generous gift from Dr. S Harper (AstraZeneca R&D Charnwood, Loughborough, U.K.).

HLMC purification

HLMC were dispersed from macroscopically normal lung obtained within 1 h of resection for lung cancer as described previously (13). Mast cells were purified using immunomagnetic affinity selection with antimouse IgG1 magnetic beads coated with the mouse anti-c-kit mAb YB5.B8 (13). Final mast cell purity was >99% and viability >97%.

Following purification, HLMC were cultured overnight on 1% BSA-coated plastic (to prevent adhesion) in RPMI 1640/Glutamax/HEPES containing antibiotic/antimycotic solution, nonessential amino acids, 10% FCS, and 10 ng/ml SCF. Cells were sensitized with human myeloma IgE (2.5 μg/ml) as required.

Primary mast cell culture from human adult peripheral blood

Mast cells were grown from progenitors in adult peripheral blood using a modification of the method described by Saito et al. (14) for human cord blood. Briefly, the mononuclear fraction from 150 ml adult peripheral blood was isolated on Histopaque, incubated for 1 h at 37°C to remove adherent cells, and then cultured in RPMI 1640/HEPES containing 5% heat-inactivated pooled human serum, SCF (100 ng/ml), IL-6 (50 ng/ml), and IL-10 (10 ng/ml). Half the medium was replaced with fresh medium every 7 days. Mast cells cultured this way are functionally mature by 3 wk in culture in terms of histamine, leukotriene C_4 (LTC_4), tryptase, and cytokine release in response to IgE-dependent activation (Refs. 15–19 and our unpublished data). After 6 wk of culture, ~50% of cells are mast cells based on metachromatic staining. For electrophysiological recording and study of mediator release, the mast cell population after 6 wk was purified using immunomagnetic affinity selection as described above for HLMC, providing a 100% pure population of mast cells. These were used in experiments for another 4 wk.

Cell viability

Mast cell viability, monitored by exclusion of trypan blue, was >97% in all experiments.

Electrophysiology

The whole-cell variant of the patch clamp technique was used (20). Patch pipettes were made from boro-silicate fiber-containing glass (Clark Electromedical Instruments, Reading, U.K.), and their tips were heat polished, resulting in resistances of typically 4–6 MΩ. The standard pipette solution contained 140 mM KCl, 2 mM $MgCl_2$, 5 mM EGTA, and 10 mM HEPES (pH 7.3). The standard external solution contained 140 mM NaCl, 5 mM KCl, 2 mM $CaCl_2$, 1 mM $MgCl_2$, and 10 mM HEPES (pH 7.3). These and other solutions used are shown in Table I. For recording, mast cells were placed in 35-mm dishes containing standard external solution.

Whole-cell currents were recorded using an Axoclamp 200A amplifier (Axon Instruments, Foster City, CA) and currents usually evoked by applying voltage commands to a range of potentials in 10-mV steps from a holding potential of −20 mV. The currents were digitized (sampled at a frequency of 10 kHz), stored on computer, and subsequently analyzed using pClamp software version 7 (Axon Instruments). Capacitance transients were minimized using the capacitance neutralization circuits on the amplifier. Correction for series resistance was not routinely applied. Junction potential changes during Cl^- substitution experiments were measured. These were found to be no >3 mV and were ignored during analysis. Experiments were performed at 27°C (HLMC) and 29°C (HPBDMC), temperature being controlled by a Peltier device. Experiments were performed with a perfusion system (Automate Scientific, San Francisco, CA) to allow solution changes, although drugs were added directly to the recording chamber. To monitor changes in cell membrane potential, data were acquired in current clamp mode.

Mast cell mediator release

For analysis of histamine and LTC_4 release, 1–2 × 10^4 mast cells were warmed to 37°C in 50 μl of culture medium in duplicate, and an equal volume of culture medium containing sheep anti-human IgE at twice the final concentration was added. After a 45-min incubation at 37°C, 100 μl of ice-cold medium was added and the cells were centrifuged at 500 × *g* for 4 min to pellet the cells. The supernatant was decanted, and control cell pellets were lysed in sterile deionized water for measurement of total histamine content. ChTX was preincubated with the cells for 10 min before activation where appropriate.

Histamine and LTC_4 assay

Histamine was measured by a sensitive radioenzymic assay based on the conversion of histamine to [^{3}H]methylhistamine in the presence of the enzyme histamine-*N*-methyltransferase using *S*-adenosyl-L-[*methyl*-^{3}H]methionine as the methyl donor (13, 21). Histamine secretion is expressed as a percentage of total cellular content (cell lysate plus spontaneous release) and is corrected for spontaneous release. LTC_4 was measured by ELISA according to the manufacturer's instructions (Amersham Pharmacia Biotech, Uppsala, Sweden).

Data presentation and statistical analysis

Data are expressed as mean ± SEM unless otherwise stated. Differences between groups of data were explored using Student's paired or unpaired *t* test (two tailed) as appropriate. A $p < 0.05$ was considered to be statistically significant.

Results

Resting ionic currents in HPBDMC

Two-thirds of HPBDMC (44 of 64 cells from 3 donors) were electrically silent at rest, with resting membrane potential around 0 mV. Of the remaining cells, 17 expressed small outwardly rectifying currents which often underwent irreversible "rundown" within the first minute of achieving the whole-cell configuration and with reversal potential and resting membrane potential of 0 mV suggesting a probable Cl^- conductance. Three cells demonstrated a K^+ current that was otherwise seen to develop acutely after IgE-dependent activation but never spontaneously in control cells recorded for 10 min (see below).

IgE-dependent ion currents in HPBDMC

HPBDMC were consistent in their response to IgE-dependent activation, and seals generally remained stabile during activation and solution changes. In 28 of 33 cells from 3 donors recorded at 29°C (extracellular solution E1, pipette solution I2, Table I), there was an acute negative shift in membrane potential from a baseline mean −4.4 ± 3.14 mV to −43.6 ± 3.1 mV within 2 min of adding anti-IgE (1/1000 dilution of stock polyclonal IgG fraction which gives optimal histamine release) to the bath (Fig. 1*A; p* < 0.0001 for all 33 cells). This was associated with the rapid development of a whole-cell current (3.5 ± 0.6 pA at baseline, 28.6 ± 4.5 pA after

Table I. *Ionic composition of commonly used solutions*[a]

Solution	NaCl (mM)	KCl (mM)	Na-Meth (mM)	K-Meth (mM)	$CaCl_2$ (mM)	$MgCl_2$ (mM)	EGTA (mM)
E1	140	5			2	1	
E2	5	140			2	1	
E3	140	5				3	
E4		5	140		2	1	
E5		5	140			3	
I1		140				2	5
I2		140				2	0.2
I3		140				2	

[a] All solutions contained 10 mM HEPES and were buffered to pH 7.3. Osmolarity was adjusted to 300 mOsM using glucose as necessary. E, Extracellular bath solution; I, intracellular pipette solution; Meth, methanesulfonate.

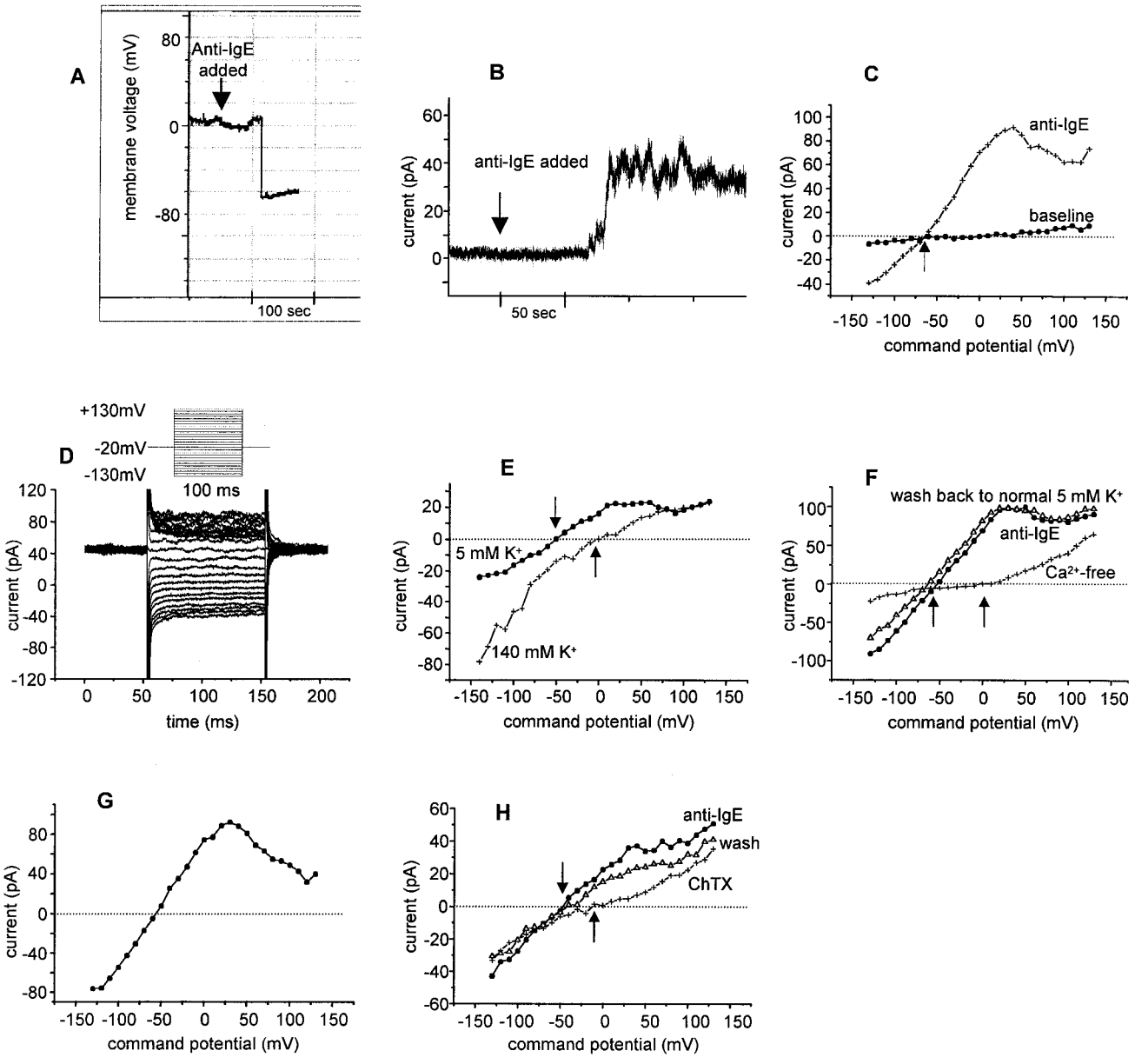

FIGURE 1. Whole-cell electrophysiological recording of membrane potential and electrical currents in HPBDMC at rest and following IgE-dependent activation. *A*, Continuous recording of membrane potential in current-clamp mode demonstrating a resting membrane potential around +5 mV, with an acute negative shift to −60 mV within 1 min of adding anti-IgE to the bath solution. *B*, Continuous recording of current at +30 mV in another cell demonstrating a rapid increase in outward current within 90 s of adding anti-IgE to the recording chamber. *C*, Current-voltage curves from another cell at rest and 2 min after IgE-dependent activation. The cell is electrically silent at baseline with no current present. Following addition of anti-IgE to the bath, a linear current develops which demonstrates rectification at positive potentials. Note the negative shift in reversal potential to −70 mV (arrow), indicating that the current is likely to be carried predominantly by K^+. *D*, Raw current from the same cell as in *C* after anti-IgE demonstrating appearance of current immediately following voltage steps and no decay during a 100-ms pulse. The voltage protocol as described in the text is shown in the *inset*. *E*, Another cell after anti-IgE recorded in 5 and 140 mM external K^+. Inward current increases, outward current decreases, and reversal potential shifts from −50 to 0 mV (arrows) on switching from 5 to 140 mM external K^+, confirming the presence of a K^+ current. Note also the inward rectification in 140 mM K^+. *F*, Another cell after anti-IgE demonstrating the typical whole-cell current. Following removal of extracellular Ca^{2+}, there is a marked and fully reversible decrease in the whole-cell current with a shift in reversal potential from −55 to 0 mV (arrows), indicating that the K^+ component is carried by a K_{CA}. A smaller outwardly rectifying Ca^{2+}-insensitive current remains; the reversal potential of 0 mV suggests it is likely to be carried by Cl^- (see Fig. 2). *G*, The Ca^{2+}-sensitive component of the whole-cell current in *E* obtained by subtraction of the calcium-insensitive component. There is marked inward rectification. *H*, Another cell after anti-IgE-dependent activation before and after addition of 100 nM ChTX. The current is decreased and reversal potential shifts from −45 to −10 mV, indicating partial blockade of the K^+ current. The effect is partially reversible on removing the ChTX.

anti-IgE at +30 mV, $p < 0.0001$ for all 33 cells) which reached a peak within 20 s of first appearing (Fig. 1*B*). The current appeared immediately as voltage steps were applied, did not decay during a 100-ms pulse (Fig. 1, *C* and *D*), and demonstrated inward rectification from membrane potentials positive to about +20 mV (Fig. 1, *C* and *D*). Reversal potential of this whole-cell current always correlated very closely with the measured membrane potential. This current was carried predominantly by K^+ ions as demonstrated by a positive shift in reversal potential to 0 mV on switching from 5 mM external K^+ to 140 mM external K^+ (14 of 14 cells; solution E2), and under these conditions was observed to exhibit weak inward rectification (Fig. 1*E*). The current was

dependent on the presence of extracellular Ca^{2+} since either switching to Ca^{2+}-free extracellular bath solution (solution E3) or adding 5 mM EGTA to the bath eliminated the K^+ conductance and shifted reversal potential to 0 mV in a fully reversible manner (5 of 5 and 3 of 3 cells respectively) (Fig. 1, *F* and *G*). This Ca^{2+}-activated K^+ current (K_{CA}) persisted for up to 45 min of recording in the whole-cell configuration with minimal rundown during this period. When recording cells that had been activated with anti-IgE for up to 30 min before achieving the whole-cell patch clamp configuration, the same current was present immediately on achieving the whole-cell configuration in 9 of 10 cells, indicating that this current did not develop as an artifact of patch clamp recording. In 4 cells, the whole-cell K^+ current demonstrated more marked inward rectification (e.g., Fig. 1*B*), which may have been highlighted by the absence of a significant Cl^- current (see below).

In six of nine cells expressing the K_{CA} current after anti-IgE, ChTX, a blocker of the intermediate conductance Ca^{2+}-activated K^+ channel hIKCA1 (hSK4/hsKCA4/hIK1) (22–25), produced a dose-dependent and reversible depolarization in 5 mM external K^+ (ChTX concentration range, 10–100 nM). At a concentration of 30 nM, reversal potential shifted from -38.7 ± 2.9 to -11.2 ± 0.8 mV in six of nine cells ($p = 0.003$ for all nine cells tested) (Fig. 1*G*). This was matched by a decrease in current from 23.9 ± 4.9 to 6.0 ± 1.2 pA at +30 mV ($p = 0.003$ for all nine cells tested). In the three other cells, in which the K_{CA} was relatively large and demonstrated more marked inward rectification, ChTX had much less effect in two and no effect in one. Because complete depolarization was always observed when extracellular Ca^{2+} was removed, this suggests the presence of a second ChTX-insensitive K_{CA} channel contributing to the hyperpolarizing potential. Apamin, a blocker of small conductance K_{CA}s had no effect on two cells, but produced a marked and partially reversible block in a third cell (data not shown), which lends some support to this suggestion. Adding ChTX to the bath before adding anti-IgE prevented membrane hyperpolarization, which then appeared on washout of the ChTX (data not shown). Addition of 30 μM barium was without effect on the K^+ current, excluding a contribution from a classical Kir channel, but 300 μM barium produced a marked block at both positive and negative potentials and accompanying membrane depolarization ($n = 3$; data not shown).

Following elimination of the dominant K^+ current with Ca^{2+}-free extracellular solution, a smaller outwardly rectifying current with a reversal potential of 0 mV remained, suggesting the presence of either a Cl^- or mixed cation current (Fig. 2). Reducing the extracellular Cl^- concentration to 11 mM from 151 mM using a Ca^{2+}-free Na^+ methanesulfonate solution **(**solution E5 **)** produced a decrease in outward current from 36.0 ± 3.4 to 27.5 ± 4.3 pA at +130 mV ($n = 4$, $p = 0.006$) and a positive shift in reversal potential of 20.7 ± 3.0 pA ($p = 0.006$; Fig. 2*B*), indicating the presence of a Cl^- conductance not activated by Ca^{2+}. This Cl^- conductance appeared immediately following voltage steps and did not inactivate during 100-ms pulses (Fig. 2*A*).

Ion currents in HLMC at rest

The majority of HLMC (58 of 91 cells, 14 donors) were electrically silent at rest with no inward or outward current (Fig. 3*A*). Resting membrane potential in these cells hovered around 0 mV, and for all cells studied was a mean -4.4 ± 1.4 mV. In 8 of these donors, 23 of 75 cells recorded expressed outwardly rectifying currents of varying amplitude at rest with mean reversal potential of -7.4 ± 3.8 mV, suggesting these were likely to be dominated by a Cl^- conductance in the solutions used (I1, 2, 3;E1). In 8 of these cells, the current only activated positive to about +30 mV and resembled the resting whole-cell current we have recently described in the leukemic HMC-1 human mast cell line (12) both in terms of its slightly delayed activation and whole-cell current-voltage relationship (Fig. 3, *B* and *C*). Reducing the concentration of external Cl^- ions from 151 to 11 mM by switching to solution containing Na^+ methanesulfonate (solution E4) reduced outward amplitude of this current by $33.3 \pm 6.8\%$ ($n = 2$) at a command potential of +130 mV, supporting the presence of a dominant Cl^- conductance (due to activation at positive potentials, it was not possible to demonstrate the predicted positive shift in reversal potential in low Cl^- solution) (Fig. 3*C*). Increasing extracellular K^+ concentration to 140 mM in these cells was without effect (data not shown). In the other 15 cells, the resting outwardly rectifying whole-cell current appeared immediately following voltage steps and resembled the activation-dependent Cl^- conductance described above for both HPBDMC and HLMC below (Fig. 3, *D* and *E*). In 9 of 51 cells from 6 donors, small linear currents were present at rest with mean reversal potential of -21.8 ± 3.8 mV, suggesting the presence of open K^+ channels. This was confirmed by demonstrating an appropriate shift in reversal potential to 0 mV on switching to 140 mM K^+ externally ($n = 3$; Fig. 3*F*). In control

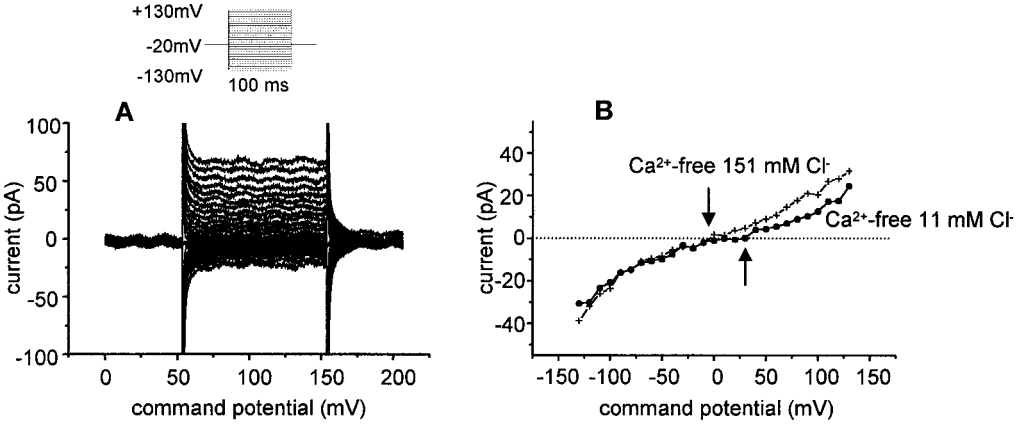

FIGURE 2. Whole-cell electrophysiological recording of electrical current in HPBDMC following IgE-dependent activation in Ca^{2+}-free recording solution. *A*, Residual raw current in Ca^{2+}-free NaCl solution, same cell as in Fig. 1*E*. Note the immediate appearance of current following voltage steps and that there is no inactivation during a 100-ms pulse. The voltage protocol as described in the text is shown in the *inset*. *B*, Current-voltage curve from another cell recorded in Ca^{2+}-free NaCl solution and then Ca^{2+}-free Na^+ methanesulfonate (11 mM Cl^-). Note the reduction in outward current and positive shift in reversal potential, indicating the presence of a Cl^- current.

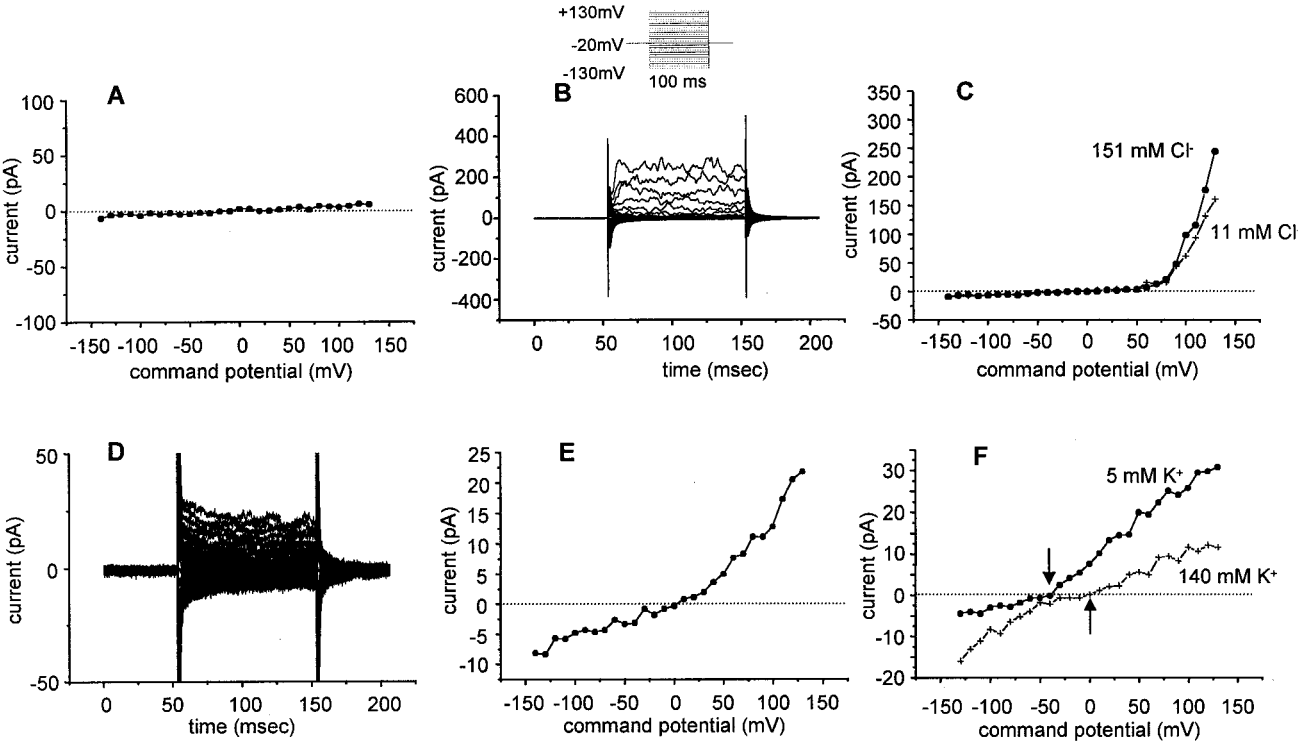

FIGURE 3. Whole-cell electrophysiological recording of HLMC showing heterogeneity of electrical currents present at rest. *A*, Current-voltage curve from an electrically silent HLMC at rest. *B*, Raw current from another cell at rest showing outward rectification and slightly delayed activation similar to that in the HMC-1 cell line. The voltage protocol as described in the text is shown in the *inset*. *C*, Current-voltage curve from the same cell as in *B* demonstrating pronounced voltage-dependent activation at around +50 mV. Switching from 151 to 11 mM extracellular Cl^- reduces the outward current, confirming the presence of a Cl^- conductance. *D* and *E*, Raw current and current-voltage curve for another cell at rest. Note the immediate appearance of current following voltage steps in *D* and weak outward rectification and reversal potential around 0 mV in *E*. Voltage protocol as in *B*. *F*, Current-voltage curve for another cell demonstrating a linear whole-cell current with reversal potential of −40 mV in 5 mM external K^+ (arrow), suggesting a dominant K^+ component. This is confirmed by switching to 140 mM external K^+ with a resulting shift to the right of the current-voltage trace and positive shift in reversal potential to 0 mV (arrow).

experiments, no cells developed currents spontaneously within 15 min of achieving the whole-cell configuration ($n = 15$).

IgE-dependent ion currents in human lung mast cells

Due to the instability of membrane seals with increasing temperature, HLMC were activated with sheep anti-human IgE at 27°C after the whole-cell configuration had been obtained. Even then, the whole-cell configuration was readily lost either spontaneously or during solution changes. In 11 of 14 donors, 18 of 41 cells responded to anti-IgE with the development of an increased whole-cell conductance. Because of the difficulty changing solutions, the calcium dependency of these anti-IgE-induced currents was determined by buffering intracellular Ca^{2+} with EGTA.

In 7 of 14 cells recorded with 5 mM internal EGTA, an outwardly rectifying whole-cell current developed slowly over 10 min following activation with anti-IgE and appeared immediately following voltage steps (Fig. 4, *A* and *B*). Current increased from a baseline 7.8 ± 1.7 to 62.5 ± 13.3 pA at +130 mV. Reversal potential in these cells was −5.7 ± 3.0 mV at baseline and −2.9 ± 2.1 mV after anti-IgE ($p = 0.51$), suggesting a dominant Cl^- conductance. This was confirmed in 2 cells by reducing the extracellular Cl^- concentration from 151 to 11 mM (solution E4; Fig. 4*C*). The appearance of this Cl^- current with 5 mM EGTA in the pipette suggests that it is activated by second messengers or cell volume but not by Ca^{2+}. In 11 of 27 cells recorded with 0.2 mM internal EGTA or no internal EGTA, whole-cell current at +130 mV increased from 34.4 ± 15.1 to 103.9 ± 29.1 pA, and membrane potential shifted in a negative direction from −5.1 ± 6.2 mV at baseline to −25.3 ± 4.3 mV following IgE-dependent activation (Fig. 4*D*). When comparing the IgE-dependent change in membrane potential between 5 mM internal EGTA (2.9 ± 4.1 mV) and 0.2 mM or no internal EGTA (-20.2 ± 5.2 mV), there was a highly significant difference ($p = 0.003$). This negative shift in membrane potential with minimal Ca^{2+} buffering compared with potent Ca^{2+} buffering suggests that K_{CA}s are also opened by IgE-dependent activation, as seen with HPBDMC above. With no EGTA in the pipette, outwardly rectifying whole-cell currents developed within 2 min of adding anti-IgE and again appeared immediately following voltage steps (Fig. 4, *E* and *F*), but did not show the inward rectification that was seen with the HPBDMC, perhaps in part due to the relatively large Cl^- component of the whole-cell current in HLMC.

Because whole-cell recording may lead to washout of intracellular second messengers and may thus influence currents which develop, cells were also activated first with anti-IgE and then the whole-cell configuration obtained. Under these conditions, 8 of 10 cells exhibited outwardly rectifying whole-cell currents ($n = 6$) or linear whole-cell currents ($n = 2$) which were present immediately after achieving the whole-cell configuration (59.7 ± 12.2 pA at +130 mV). Membrane potential in these cells was −26.6 ± 6.2 mV, which differed significantly from that in resting cells (−4.4 ± 1.4 mV, $p = 0.01$). The presence of a K^+ conductance in these cells was confirmed by switching extracellular K^+ from 5 to 140 mM, which produced a shift in reversal potential from −29.2 ± 5.1 to 0.6 ± 2.2 mV ($n = 5$; Fig. 4*G*). In 140 mM K^+, the current

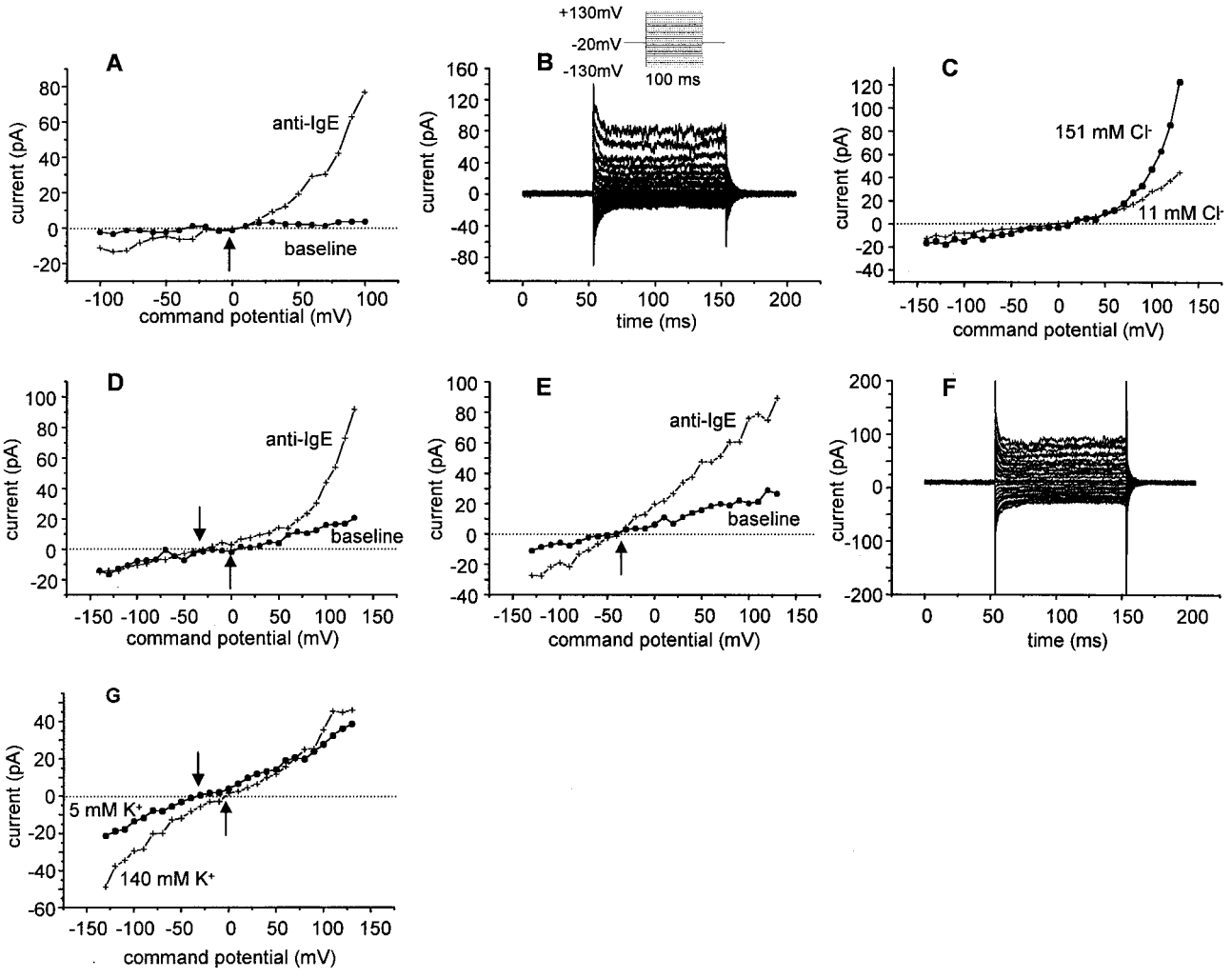

FIGURE 4. Whole-cell electrophysiological recording of ion currents in HLMC following IgE-dependent activation with differing degrees of intracellular Ca^{2+} buffering. *A*, Current-voltage curves for a HLMC recorded at rest and 10 min after IgE-dependent activation with 5 mM EGTA in the pipette. The cell is electrically silent at rest and develops an outwardly rectifying current with reversal potential of 0 mV, suggesting a dominant Cl^- conductance. The raw post-anti-IgE current in *B* appears immediately following voltage steps and does not inactivate during the 100-ms pulse. The voltage protocol as described in the text is shown in the *inset*. *C*, The post-anti-IgE outwardly rectifying current in another cell is decreased markedly by reducing extracellular Cl^- from 151 to 11 mM, indicating the presence of a Cl^- current. *D*, Current-voltage curve from a cell recorded at baseline and 5 min after activation with 0.2 mM EGTA in the pipette. Note the negative shift in reversal potential from 0 to −30 mV, suggesting the presence of both K^+ and Cl^- currents. *E*, Current-voltage curve from a cell at rest and 2 min after activation with no EGTA in the pipette. This cell demonstrates a small linear current at rest and negative reversal potential (arrow) with a marked increase in current after activation. *F*, Raw current after activation from the cell in E. This is similar to the IgE-dependent current in HPBDMC but does not rectify at positive potentials. Voltage protocol as in *B*. *G*, Current-voltage curve for a cell after activation recorded in 5 and 140 mM external K^+. Note the positive shift in reversal potential (arrows), confirming the presence of K^+ current.

demonstrated weak inward rectification similar to that seen in the HPBDMC. Furthermore, addition of 100 nM ChTX reduced current at +130 mV from 85 ± 25 to 21.8 ± 1.8 pA and produced a shift in reversal potential from −45.5 ± 12.5 to −12.5 ± 7.5 mV (n = 2), suggesting that the same K_{CA}s are expressed as in HPBDMC.

Calcium ionophore-induced currents in HLMC and HPBDMC

To further examine the presence of Ca^{2+}-activated currents in HPBDMC and HLMC, cells were incubated with the calcium ionophore A23187 (1 μM). Within 2 min of adding A23187 to the bath solution, a robust outwardly rectifying whole-cell current developed in all cells recorded when the patch pipette contained 0.2 mM EGTA (HPBDMC, n = 4; HLMC, n = 17; Fig. 5, *A–D*). No current developed when the pipette contained 5 mM EGTA (HLMC, n = 4) or when the cells were bathed in Ca^{2+}-free extracellular solution (HLMC, n = 4), indicating that the Ca^{2+} ionophore-induced current was Ca^{2+} dependent. In HLMC, current increased from a baseline 9.6 ± 1.9 to 179.8 ± 30.2 pA at +130 mV and in HPBDMC increased from a baseline 13.7 ± 4.3 to 241 ± 71.2 pA. Interestingly, in both cell types, this current had different characteristics to the IgE-dependent currents described above in that it activated slowly, suggesting it was carried by a distinct set of channels (Fig. 5, *A* and *C*). Mean reversal potentials for the currents in HLMC and HPBDMC were −2.9 ± 3.4 and −4.0 ± 9.5 mV, respectively, suggesting the presence of a dominant Cl^- conductance. This was confirmed in ion substitution experiments with current at +130 mV falling from 90 ± 20 to 31 ± 7 pA and reversal potential shifting from −7.5 ± 2.5 to 30 ±

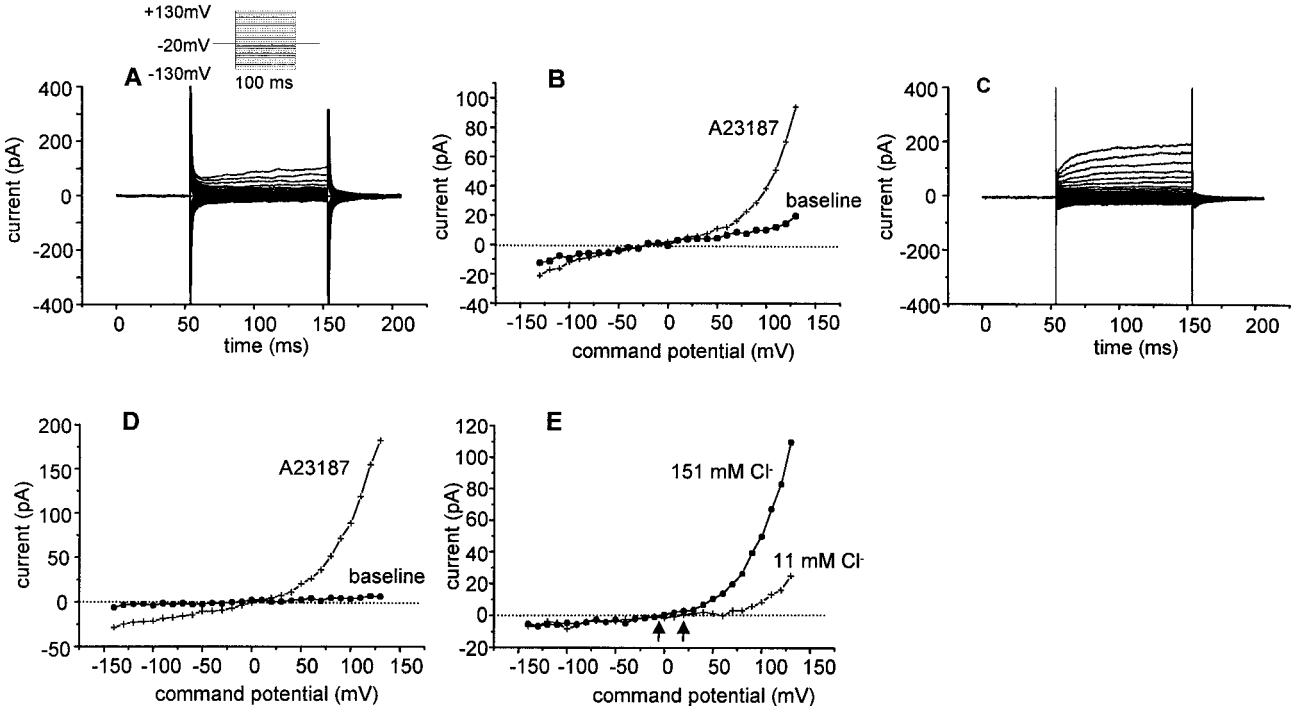

FIGURE 5. Whole-cell electrophysiological recording of ion currents in HPBDMC and HLMC following activation with the calcium ionophore A23187. *A* and *C*, Raw current from a HPBDMC and HLMC, respectively, after activation. Note the increasing activation over the duration of the test pulse, indicating that this current is carried by different channels to those activated by anti-IgE. The voltage protocol as described in the text is shown in the *inset*. *B* and *D*, Current-voltage curves from the same respective cells at baseline and following activation demonstrating strong outward rectification and reversal potential around 0 mV, suggesting a dominant Cl^- conductance. *E*, Another HLMC after A23187 recorded in 151 and 11 mM external Cl^-. The decrease in current and positive shift in reversal potential on switching to 11 mM Cl^- confirms the presence of a dominant Cl^- conductance.

10 mV following replacement of extracellular Cl^- with methanesulfonate (HLMC, $n = 2$) (Fig. 5*E*). In contrast, increasing extracellular K^+ was without effect (HLMC, $n = 2$; data not shown).

IgE-dependent K_{CA} currents and mediator release

To study the role of K_{CA} activation in HLMC and HPBDMC secretion, cells were activated with anti-IgE (1/1000 dilution **)** in the presence of ChTX (1, 10, 100 nM). Mean net histamine release from HLMC from 10 donors was 11.7 ± 3.0% (range, 0–26.6% **)**. In 6 of 7 experiments with >7% net histamine release, ChTX produced a variable but dose-dependent inhibition of this (range, 11.4–80.5% maximal inhibition; Fig. 6). Mean net histamine release from HPBDMC from 3 donors was 45.3 ± 7.51.3% ($p = 0.05$ compared with HLMC). In one experiment with HPBDMC, 100 nM ChTX produced a 33% inhibition of release, but had no effect in 2 additional experiments.

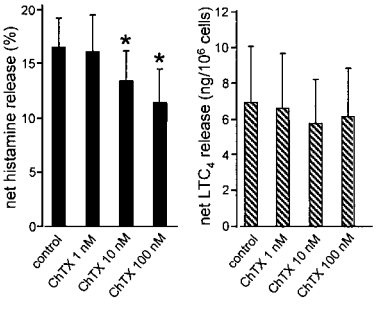

FIGURE 6. Net release of histamine (*left graph*) and LTC_4 (*right graph*) following IgE dependent of HLMC in either control buffer or increasing concentrations of ChTX (mean ± SEM of seven experiments for histamine, six experiments for LTC_4). *, $p < 0.05$ compared with control.

LTC_4 secretion from 6 experiments with HLMC that exhibited significant histamine release was a mean 7.0 ± 3.1 ng/10^6 cells. In 4 of 6 of experiments, ChTX produced a variable dose-dependent inhibition of LTC_4 release, which was always less than the inhibition of histamine release from the same cells (Fig. 6). In one experiment using HPBDMC, there was no inhibition of LTC_4 release (9.6 ng/10^6 cells) by ChTX.

Discussion

In this study, we have used the whole-cell variation of the patch clamp technique to investigate ion currents in the plasma membrane of both HLMC and HPBDMC, both at rest and following cellular activation with anti-IgE and Ca^{2+} ionophore. Despite extensive literature concerning the conductive properties of rodent mast cells, to our knowledge this is the first study of ion channel activity in functionally mature human mast cells.

In rodent mast cells, Ca^{2+}, K^+, Cl^-, and Na^+ conductances have been identified using patch clamp recording, although the role of these in cellular responses remains poorly defined. Interestingly, currents vary between different rodent mast cell phenotypes, which may explain in part mast cell functional heterogeneity (26). For example, the RBL cell line and rodent BMMC, which are considered to represent a mucosal mast cell phenotype, express a strong inwardly rectifying K^+ current at rest which is probably carried by subtype Kir2.1 channels (7) and which sets a stable resting membrane potential close to the K^+ reversal potential at about −70 mV. In contrast, rat peritoneal mast cells (RPMC), typical of connective tissue-type mast cells, are either electrically silent at rest or express an outwardly rectifying Cl^- conductance (27). RPMC release their histamine explosively within 2 min of IgE-dependent activation (28) unlike rodent "mucosal" mast cells which secrete histamine in a linear fashion over 30 min (29). It is therefore of

interest that HLMC, which degranulate rapidly with a $t_{1/2}$ for histamine release of 2 min following IgE-dependent activation (30), but which are located at a mucosal surface, and the phenotypically similar HPBDMC (15–17) are very similar to RPMC in terms of the ion currents expressed at rest.

Following IgE-dependent activation, there was an acute negative shift in membrane potential due to the opening of K_{CA}s. This was most striking in the HPBDMC but also evident in the HLMC. This is the first electrophysiological evidence of a K_{CA} in a mast cell from any species although Ca^{2+}-dependent K^+ efflux has been observed in RBL cells using $^{86}Rb^+$ as a tracer (31). The inward rectification in high extracellular K^+ and significant block by ChTX suggest that this K^+ current is carried predominantly by the intermediate conductance Ca^{2+}-activated K^+ channel hIKCA1 (hsKCA4/hSK4/hIK1) or a closely related as yet unidentified family member (22–25). Expressed hIKCA1 clones from human placental, lymph node, and pancreatic cDNA libraries demonstrate electrophysiological features virtually identical to the currents we have observed in both types of human mast cell, as well as those described for other hemopoietic cells, including T cells (22, 32) and macrophage/monocytes (33). The negative shift in membrane potential resulting from opening of these channels will increase Ca^{2+} influx both by increasing the electrical driving force for Ca^{2+} entry, but perhaps more importantly by increasing the open probability of the SOCC. These latter channels that carry Ca^{2+} into the cell demonstrate inward rectification at negative potentials (9), and thus carry larger Ca^{2+} currents at negative potentials. This would therefore be predicted to increase mediator release and influence Ca^{2+}-dependent gene transcription.

Indirect evidence supporting a prosecretory role for K_{CA} channel opening in mast cells is provided by the observation that our HPBDMC, in which the K_{CA} current predominates, and blood-derived mast cells cultured by other workers using similar methods, release ~40% of total cellular histamine (Refs. 15 and 16, and our unpublished data), whereas HLMC, in which the K_{CA} current is less marked, show marked heterogeneity releasing 0–30% of total cellular histamine. However, although ChTX produced a significant block of the whole-cell current, the effect on histamine and LTC_4 release was clearly very variable in HLMC and minimal in HPBDMC. There may be several explanations for this observation. Although ChTX depolarized activated cells, membrane potential after the addition of ChTX was still usually more negative (approximately −10 mV) than the resting value preactivation (~0 mV). This would still provide some driving force for Ca^{2+} influx although the magnitude of the Ca^{2+} current would be predicted to be reduced. This persisting polarization suggests that we may have incompletely blocked the ChTX-sensitive channels, that some degradation of ChTX may have taken place due to the release of mast cell proteases and reactive oxygen species, particularly during mediator release experiments where cell number is higher, or that a second type of K_{CA} channel resistant to ChTX is present. The latter is plausible because ChTX had little effect on the K^+ current in some cells and apamin, a blocker of the small conductance K_{CA} channels hsKCA2 and 3, produced reversible inhibition of the whole-cell current in one of three cells tested. Thus, depolarization required to attenuate secretion may not have been consistently achieved. Another consideration is that K_{CA} activity is more important for distal responses such as Ca^{2+}-dependent gene transcription, because in T cells, hIKCA1 blockade with ChTX inhibits cell proliferation and IFN-γ production (34). Finally, hIKCA1 also plays a role in cell volume regulation in T cells (25), which is therefore another potential role for the K_{CA} channel in degranulating mast cells.

In addition to the K_{CA} current identified, immunological activation in both HPBDMC and HLMC also opened at least one Cl^- channel which was not dependent on Ca^{2+} influx. This current was isolated by recording HPBDMC in Ca^{2+}-free extracellular recording solution and HLMC with high intracellular EGTA. It appeared slowly over 10 min following activation, was outwardly rectifying, and appeared immediately following voltage steps with no decay over a 100-ms pulse. A similar current of lower amplitude was present in some cells at rest and may be carried by the same channels, but the current never developed spontaneously after achieving the whole-cell configuration, and in HPBDMC usually ran down rapidly if present at baseline. This indicates that the current appeared as a result of cell activation and not as an artifact of patch clamp recording. A similar current is present in a proportion of rat peritoneal and BMMC at rest (27) and also develops slowly in these and RBL cells after IgE-dependent activation (10, 35). Interpreting the role of this Cl^- current during cell activation is difficult because the intracellular Cl^- concentration, which varies widely between cells, is not known for human mast cells. The physiological extracellular Cl^- concentration is ~100 mM, so if the intracellular Cl^- concentration is in the region of 30 mM as has been estimated for RPMC (36), Cl^- currents will contribute to membrane polarization since reversal potential for Cl^- at these concentrations is about −40 mV, and this will theoretically promote Ca^{2+} influx. In support of this, blockers of rodent mast cell Cl^- channels such as 5-nitro-2-(3-phenylpropylamino)benzoic acid (NPPB) and 4,4′-diisothiocyanato-2,2′-disulfonic acid (DIDS) attenuate histamine secretion but only in the micromolar range (36, 37). However, NPPB also inhibits Ca^{2+} influx through SOCC (37), and although DIDS attenuates secretion and blocks Cl^- channels, it does not inhibit Ag-induced $^{36}Cl^-$ uptake in RPMC which occurs rapidly, while the appearance of Cl^- channel activity is delayed (36). Furthermore, although sodium cromoglycate is a potent blocker of the IgE-dependent Cl^- conductance in RBL cells (10), it is only a weak antagonist of secretion from HLMC. Thus, the role of the delayed Cl^- current in rodents remains unclear. Conversely, if the intracellular Cl^- concentration in HLMC is similar to the extracellular Cl^- concentration, then Cl^- channel opening will depolarize the cell and antagonize Ca^{2+} influx. With this scenario, one could hypothesize that since the appearance of this current is delayed following activation, it actually represents a negative feedback pathway to provide a brake to the secretory response.

Most cells express Cl^- channels that are believed to be important for the regulation of cell volume. Two members of the voltage-dependent family of Cl^- channels, namely, the inwardly rectifying channel ClC-2 and the outwardly rectifying channel ClC-3, are widely expressed in mammalian cells and activate in response to reduced extracellular osmolarity. Currents carried through ClC-3 have similar physiological characteristics to the Cl^- currents expressed in HLMC and HPBDMC, suggesting that this channel may carry the IgE-dependent Cl^- current. The primary role of this current may therefore be to regulate cell volume following activation, perhaps in concert with the K_{CA}. Firm molecular identification of the channels present and selective inactivation, for example, with antisense oligodeoxynucleotides, will answer these questions.

A second type of Cl^- current was activated by Ca^{2+} influx in both HPBDMC and HLMC following exposure to the calcium ionophore A23187. This current may also have contributed to the whole-cell current following IgE-dependent activation, but if so was masked by the K^+ and delayed Cl^- currents. The A23187-induced current was clearly different from the other currents in terms of its activation kinetics, indicating it is carried by a distinct

set of channels, and was very similar to the Ca^{2+}-activated Cl^- current described previously in other cell types including human neutrophils (38). It is interesting that this current was dominant after A23187-induced activation, with little evidence of the K_{CA} current, whereas the K_{CA} current was more pronounced following IgE-dependent activation. To some extent the relatively large ionophore-induced current may have hidden the smaller K_{CA} current, but the correct intracellular signals following IgE-dependent activation may also have a critical role in permitting mast cell K_{CA} opening, as phosphorylation, for example, is known to affect K_{CA} channel gating (39). Similar observations have been made in neutrophils which also express K_{CA} channels, but develop a dominant Cl^- current similar to the mast cell current in response to calcium ionophore (38).

In this study, we have used the whole-cell configuration of the patch clamp technique to analyze HPBDMC and HLMC ion currents. As the cell is dialyzed by the pipette solution, there is the potential for washout of important intracellular constituents such as cyclic nucleotides which may themselves modulate ion channel function. Thus, it is possible that these cells express further currents which have not been identified in this study. Further analysis using the perforated patch technique will help address this. In addition, recording was limited to a temperature of 27–29°C because of the instability of seals at greater temperatures. Because mast cell activation and Ca^{2+} influx are temperature dependent and maximal at 37°C (40, 41), it is likely that the magnitude of Ca^{2+}-activated currents is attenuated under our recording conditions and the time course of channel activation slowed.

In summary, we have described for the first time ion currents present in functionally mature human mast cells. Interestingly there is little electrical activity at rest, but immediately after IgE-dependent activation there is opening of a K_{CA}, likely to be hIKCA1, which results in membrane hyperpolarization, and this is followed by opening of a calcium-independent Cl^- channel. Specific molecular identification and knockout of these channels will permit accurate assessment of their role in human mast cell biology. Finally, we need to study tissue mast cells recovered from patients with specific diseases such as asthma to understand the role of these and other ion channels in mast cell disease. Ultimately, this may lead to novel therapeutic strategies based on modulation of human mast cell ion channel activity.

Acknowledgments

We are very grateful to Dr. S. Harper (AstraZeneca R&D Charnwood, Loughborough, U.K.) for performing the LTC_4 assay.

References

1. Bradding, P. 2000. Mast cells in asthma. In *Asthma & Rhinitis*, 2nd Ed. W. W. Busse and S. T. Holgate, eds. Blackwell, Boston, p. 319.
2. Bradding, P., and S. T. Holgate. 1999. Immunopathology and human mast cell cytokines. *Crit. Rev. Oncol. Hematol. 31:119.*
3. Lin, C. S., R. C. Boltz, J. T. Blake, M. Nguyen, A. Talento, P. A. Fischer, M. S. Springer, N. H. Sigal, R. S. Slaughter, and M. L. Garcia. 1993. Voltage-gated potassium channels regulate calcium-dependent pathways involved in human T lymphocyte activation. *J. Exp. Med.177:637.*
4. Koo, G. C., J. T. Blake, A. Talento, M. Nguyen, S. Lin, K. Sirotina, K. Shah, D. J. Mulvany, P. Hora, D. L. Cunningham, et al. 1997. Blockade of the voltage-gated potassium channel Kv1.3 inhibits immune responses in vivo. *J. Immunol. 158:5120.*
5. Lindau, M., and J. M. Fernandez. 1986. A patch-clamp study of histamine-secreting cells. *J. Gen. Physiol. 88:349.*
6. McCloskey, M. A., and Y. X. Qian. 1994. Selective expression of potassium channels during mast cell differentiation. *J. Biol. Chem. 269:14813.*
7. Wischmeyer, E., K. U. Lentes, and A. Karschin. 1995. Physiological and molecular characterization of an IRK-type inward rectifier K^+ channel in a tumour mast cell line. *Pflügers Arch. Eur. J. Physiol. 429:809.*
8. Fasolato, C., M. Hoth, G. Matthews, and R. Penner. 1993. Ca^{2+} and Mn^{2+} influx through receptor-mediated activation of nonspecific cation channels in mast cells. *Proc. Natl. Acad. Sci. USA 90:3068.*
9. Hoth, M., and R. Penner. 1992. Depletion of intracellular calcium stores activates a calcium current in mast cells. *Nature 355:353.*
10. Romanin, C., M. Reinsprecht, I. Pecht, and H. Schindler. 1991. Immunologically activated chloride channels involved in degranulation of rat mucosal mast cells. *EMBO J. 10:3603.*
11. Qian, Y. X., and M. A. McCloskey. 1993. Activation of mast cell K^+ channels through multiple G protein-linked receptors. *Proc. Natl. Acad. Sci. USA 90:7844.*
12. Duffy, S. M., M. L. Leyland, E. C. Conley, and P. Bradding. 2001. Voltage-dependent and calcium-activated ion channels in the human mast cell line HMC-1. *J. Leukocyte Biol. 70:233.*
13. Sanmugalingam, D., A. J. Wardlaw, and P. Bradding. 2000. Adhesion of human lung mast cells to bronchial epithelium: evidence for a novel carbohydrate-mediated mechanism. *J. Leukocyte Biol. 68:38.*
14. Saito, H., M. Ebisawa, H. Tachimoto, M. Shichijo, K. Fukagawa, K. Matsumoto, Y. Iikura, T. Awaji, G. Tsujimoto, M. Yanagida, et al. 1996. Selective growth of human mast cells induced by Steel factor, IL-6, and prostaglandin E_2 from cord blood mononuclear cells. *J. Immunol. 157:343.*
15. Valent, P., E. Spanblochl, W. R. Sperr, C. Sillaber, K. M. Zsebo, H. Agis, H. Strobl, K. Geissler, P. Bettelheim, and K. Lechner. 1992. Induction of differentiation of human mast cells from bone marrow and peripheral blood mononuclear cells by recombinant human stem cell factor/kit-ligand in long-term culture. *Blood 80:2237.*
16. Igarashi, Y., M. Kurosawa, O. Ishikawa, Y. Miyachi, H. Saito, M. Ebisawa, Y. Iikura, M. Yanagida, H. Uzumaki, and T. Nakahata. 1996. Characteristics of histamine release from cultured human mast cells. *Clin. Exp. Allergy 26:597.*
17. Shichijo, M., N. Inagaki, N. Nakai, M. Kimata, T. Nakahata, I. Serizawa, Y. Iikura, H. Saito, and H. Nagai. 1998. The effects of anti-asthma drugs on mediator release from cultured human mast cells. *Clin. Exp. Allergy 28:1228.*
18. Bressler, R. B., J. Lesko, M. L. Jones, M. Wasserman, R. R. Dickason, M. M. Huston, S. W. Cook, and D. P. Huston. 1997. Production of IL-5 and granulocyte-macrophage colony-stimulating factor by naive human mast cells activated by high-affinity IgE receptor ligation. *J. Allergy Clin. Immunol. 99:508.*
19. Toru, H., R. Pawankar, C. Ra, J. Yata, and T. Nakahata. 1998. Human mast cells produce IL-13 by high-affinity IgE receptor cross-linking: enhanced IL-13 production by IL-4-primed human mast cells. *J. Allergy Clin. Immunol. 102:491.*
20. Hamill, O. P., A. Marty, E. Neher, B. Sakmann, and F. J. Sigworth. 1981. Improved patch-clamp techniques for high-resolution current recording from cells and cell-free membrane patches. *Pflügers Arch. Eur. J. Physiol. 391:85.*
21. Snyder, S. H., R. J. Baldessarini, and J. Axelrod. 1966. A sensitive and specific enzymatic isotopic assay for tissue histamine. *J. Pharmacol. Exp. Ther. 153:544.*
22. Logsdon, N. J., J. Kang, J. A. Togo, E. P. Christian, and J. Aiyar. 1997. A novel gene, hKCa4, encodes the calcium-activated potassium channel in human T lymphocytes. *J. Biol. Chem. 272:32723.*
23. Ishii, T. M., C. Silvia, B. Hirschberg, C. T. Bond, J. P. Adelman, and J. Maylie. 1997. A human intermediate conductance calcium-activated potassium channel. *Proc. Natl. Acad. Sci. USA 94:11651.*
24. Jensen, B. S., D. Strobaek, P. Christophersen, T. D. Jorgensen, C. Hansen, A. Silahtaroglu, S. P. Olesen, and P. K. Ahring. 1998. Characterization of the cloned human intermediate-conductance Ca^{2+}-activated K^+ channel. *Am. J. Physiol. 275:C848.*
25. Khanna, R., M. C. Chang, W. J. Joiner, L. K. Kaczmarek, and L. C. Schlichter. 1999. hSK4./hIK1, a calmodulin-binding KCa channel in human T lymphocytes: roles in proliferation and volume regulation. *J. Biol. Chem. 274:14838.*
26. Church, M. K., Y. Okayama, and P. Bradding. 1994. Functional mast cell heterogeneity. In *Asthma and Rhinitis*, W. W. Busse and S. T. Holgate, eds. Blackwell, Boston, p. 209.
27. Hill, P. B., R. J. Martin, and H. R. Miller. 1996. Characterization of whole-cell currents in mucosal and connective tissue rat mast cells using amphotericin-B-perforated patches and temperature control. *Pflügers Arch. Eur. J. Physiol. 432: 986.*
28. Schwartz, L. B., K. F. Austen, and S. I. Wasserman. 1979. Immunologic release of β-hexosaminidase and β-glucuronidase from purified rat serosal mast cells. *J. Immunol. 123:1445.*
29. MacDonald, A. J., D. M. Haig, H. Bazin, A. C. McGuigan, R. Moqbel, and H. R. Miller. 1989. IgE-mediated release of rat mast cell protease II, β-hexosaminidase and leukotriene C4 from cultured bone marrow-derived rat mast cells. *Immunology 67:414.*
30. Schleimer, R. P., D. W. MacGlashan, Jr., S. P. Peters, R. N. Pinckard, N. F. Adkinson, Jr., and L. M. Lichtenstein. 1986. Characterization of inflammatory mediator release from purified human lung mast cells. *Am. Rev. Respir. Dis. 133:614.*
31. Labrecque, G. F., D. Holowka, and B. Baird. 1991. Characterization of increased K^+ permeability associated with the stimulation of receptors for immunoglobulin E on rat basophilic leukemia cells. *J. Biol. Chem. 266:14912.*
32. Grissmer, S., A. N. Nguyen, and M. D. Cahalan. 1993. Calcium-activated potassium channels in resting and activated human T lymphocytes: expression levels, calcium dependence, ion selectivity, and pharmacology. *J. Gen. Physiol. 102:601.*
33. Kim, S. Y., M. R. Silver, and T. E. DeCoursey. 1996. Ion channels in human THP-1 monocytes. *J. Membr. Biol. 152:117.*
34. Jensen, B. S., N. Odum, N. K. Jorgensen, P. Christophersen, and S. P. Olesen. 1999. Inhibition of T cell proliferation by selective block of Ca^{2+}-activated K^+ channels. *Proc. Natl. Acad. Sci. USA 96:10917.*

35. Matthews, G., E. Neher, and R. Penner. 1989. Chloride conductance activated by external agonists and internal messengers in rat peritoneal mast cells. *J. Physiol. 418:131.*
36. Friis, U. G., T. Johansen, N. A. Hayes, and J. C. Foreman. 1994. IgE-receptor activated chloride uptake in relation to histamine secretion from rat mast cells. *Br. J. Pharmacol. 111:1179.*
37. Reinsprecht, M., M. H. Rohn, R. J. Spadinger, I. Pecht, H. Schindler, and C. Romanin. 1995. Blockade of capacitive Ca^{2+} influx by Cl^{-} channel blockers inhibits secretion from rat mucosal-type mast cells. *Mol. Pharmacol. 47:1014.*
38. Krause, K. H., and M. J. Welsh. 1990. Voltage-dependent and Ca^{2+}-activated ion channels in human neutrophils. *J. Clin. Invest. 85:491.*
39. Gerlach, A. C., N. N. Gangopadhyay, and D. C. Devor. 2000. Kinase-dependent regulation of the intermediate conductance, calcium-dependent potassium channel, hIK1. *J. Biol. Chem. 275:585.*
40. WoldeMussie, E., K. Maeyama, and M. A. Beaven. 1986. Loss of secretory response of rat basophilic leukemia (2H3) cells at 40 degrees C is associated with reversible suppression of inositol phospholipid breakdown and calcium signals. *J. Immunol. 137:1674.*
41. Proud, D., D. W. J. MacGlashan, H. H. Newball, E. S. Schulman, and L. M. Lichtenstein. 1985. Immunoglobulin E-mediated release of a kininogenase from purified human lung mast cells. *Am. Rev. Respir. Dis. 132:405.*